

AN EFFICIENT DESIGN METHOD FOR OBROUND PRESSURE VESSELS AND THEIR END CLOSURES

K.P. Singh
President and CEO, Holtec International
Marlton, NJ 08053

ABSTRACT

Obround cross sections find extensive industrial use in pressure vessels and pipings. Yet guidelines for their design are not available in the published literature. The obround shape is inherently unsuitable to withstand internal pressure. Support gussets must be added to such pressure vessels to render their use economical. This paper gives a method to efficiently design a pressurised obround cross section by determining the appropriate gusset plate locations, and the associated bending stresses. Formulae to design the obround flanged end closures are also given.

PRINCIPAL NOTATION

- b semi-length of straight segment
- E Young's modulus of pipe material
- E_g Young's modulus of gusset material
- F_i restraining force at node i (Fig. 1, section A)
- I plane moment of inertia of ring about its central axis perpendicular to the plane of loading
- l distance between anchor rings
- m applied twisting couple per unit perimeter
- M bending moment at $x = 0$ (Fig. 2)
- M' bending moment at a generic point in the straight segment
- M_θ bending moment at a point in the curved segment
- n number of linear equations
- p force per unit perimeter (internal pressure times width of the ring)
- Q_i restraining force at node i (Fig. 1, section B)

- r arc radius of pipe
 U strain energy
 T twisting moment in the obround ring
 x_i coordinate of node i
 δ_i deflection of node i (Fig. 1, section A)
 Δ_i deflection of node i (Fig. 1, section B)
 η distance parameter

INTRODUCTION

Obround cross sections are quite common to pressure vessels in spite of their inherent weakness in resisting internal pressure. Obround shapes are preferred to the conventional circular type only when considerations other than mechanical strength are of overriding importance. A notable example is the use of obround nozzles at tubular heat-exchanger shell inlets to produce a favourable bundle penetration velocity profile from the standpoint of flow induced vibrations. Holding tanks and reactor tanks are sometimes made obround to provide an increased exposed surface for the contained liquid.

In spite of such significant applications of the obround cylinders, there is virtually no literature on their design method, although some design codes recognise their use.¹ An obround cross-section is highly unadapted to sustain internal pressure. The flat segments develop high bending stresses at relatively low pressures. To overcome this difficulty, longitudinal external gussets are provided on the flat segments (Fig. 1). The gussets are welded to the anchor rings located at a suitable spacing l . The

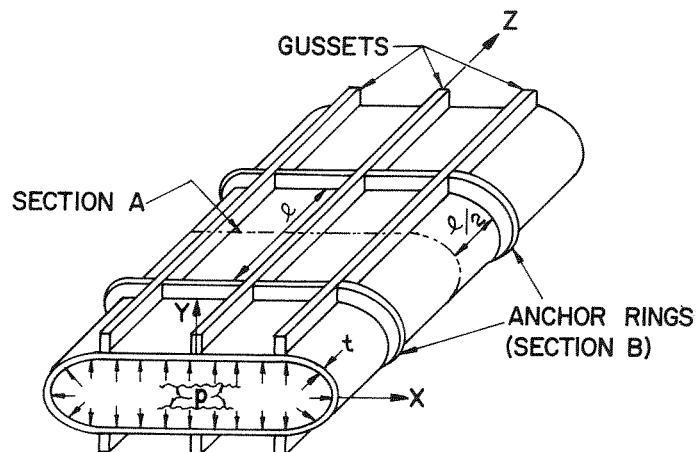


Fig. 1. Obround pipe with longitudinal gussets under internal pressure.

anchor rings together with the gussets provide the structural constraint to limit the deflection of the flat segments of the pipe. The gussets and anchor rings can be made of common structural materials such as low carbon steels,[†] whereas the pressure boundary material is often quite expensive because of its necessary corrosion resistance and other chemical properties. Thus, economics of design dictates maintaining the pressure boundary thickness to a practical minimum and finding the optimum number (and location) of gussets such that the circumferential membrane and bending stresses in the pressure vessel are held within the postulated allowable limits. The number and location of gussets and anchor rings are important design parameters. The gussets are assumed to be arranged symmetrically with respect to the x and y axes (Fig. 2). Their locations within the flat segment are otherwise completely arbitrary.

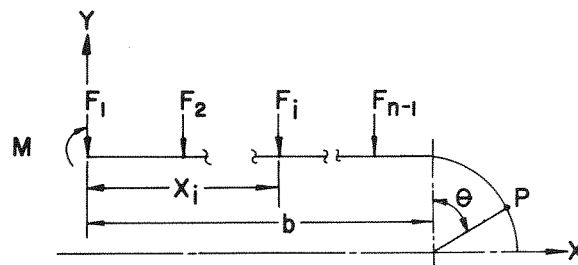


Fig. 2. Free body of ring quadrant.

Strictly speaking, the problem is three-dimensional, since the deflection of the pressure vessel will vary with z , presumably reaching a maximum at the mid-section between the anchor rings. Although a numerical solution of this problem using a suitable general purpose Finite Element computer program is feasible, such an approach is too cumbersome to be adopted as a design tool. Pressure vessel designers have long recognised the necessity of a solution technique tailored to this class of problems. This paper seeks to fulfil this need.

Attention is focused on two ring elements of the pressure vessel, located midway between the anchor rings (Section A in Fig. 1), and under the anchor ring (Section B), respectively. In the next section, a set of linear algebraic equations are derived which relate the support point forces to support deflections in a pressurised ring propped at discrete points (Fig. 2). Using this relationship in conjunction with the traction and displacement continuity requirements at Sections A and B (Fig. 1), an iterative

[†] Common gusset materials are SA36 or SA306-Gr60. The piping material in chemical applications is quite frequently austenitic stainless steel such as SA240-304 or 304L, and SA240-316 or 316L. These material designations are quoted from reference 1, Table UCS-23.

method to compute the nodal point deflections, forces, anchor ring deflection, etc., is developed.

Although the aid of a computer is required in the solution process, the actual computation effort and central core requirements are small enough to be met by a typical mini computer, for most engineering applications.

A simple method to design obround shape lap joint flanges is given later, followed by an illustrative example and concluding remarks.

OBROUND RING UNDER INTERNAL PRESSURE

Consider an obround ring of unit width arc radius r and straight segment length $2b$, subject to an internal pressure p (Fig. 2). The ring is supported at $(n - 1)$ points, referred to as 'node points', in each quadrant. The support system is symmetrical about x and y axes in Fig. 2. The support reaction at the node point i , located at a distance x_i , from the y -axis, is given by F_i , and the corresponding node point deflection is denoted by δ_i . For a completely immovable (rigid) support system all δ_i will vanish identically. The object is to derive expressions for the reactions F_i , and the moment M (at $x = 0$), for assumed values of δ_i , when the ring is subject to a specified hydrostatic pressure p .

Notice the moment M' in region K is given by:

$$M' = M - \sum_{i=1}^k F_i(x - x_i) + \frac{px^2}{2} \quad (1)$$

where the region K is defined by:

$$x_k \leq x \leq x_{k+1} \quad (2)$$

with the implied identity, $x_n = b$.

Furthermore, the moment M_θ at a point P (Fig. 2) on the curved segment is given by:

$$M_\theta = M - \sum_{i=1}^{n-1} F_i(x_n - x_i + r \sin \theta) + px_n(0.5x_n + r \sin \theta) \quad (3)$$

The gross strain energy, U , in each quadrant of the ring is given by:

$$U = \frac{1}{2EI} \left[\int_0^b M'^2 dx + r \int_0^{\pi/2} M_\theta^2 d\theta \right]$$

or

$$U = \frac{1}{2EI} \left[\sum_{k=1}^{n-1} \int_{x_k}^{x_{k+1}} M'^2 dx + r \int_0^{\pi/2} M_\theta^2 d\theta \right] \quad (4)$$

where E and I are the Young's modulus, and plane moment of inertia of ring cross section about its neutral axis, respectively.

The foregoing expression for strain energy does not contain terms due to shear and longitudinal membrane tension, which implies that the ring's cross-sectional characteristic dimensions are small compared to its geometric dimensions b and r .

Appealing to the theorem of Castigliano,^{2,3} we have

$$\frac{\partial U}{\partial F_j} = \delta_j; \quad j = 1, 2, \dots, (n-1) \quad (5)$$

Furthermore, geometric and loading symmetry requires that

$$\frac{\partial U}{\partial M} = 0 \quad (6)$$

It will be shown that eqns. (5) and (6) furnish n linear algebraic equations in n unknowns; namely $(n-1)$ elements of F_i , and the moment M .

From eqns. (4) and (5) we have:

$$\sum_{k=1}^{n-1} \int_{x_k}^{x_{k+1}} M' \frac{\partial M'}{\partial F_j} dx + r \int_0^{\pi/2} M_\theta \frac{\partial M_\theta}{\partial F_j} d\theta = \alpha_j$$

where

$$\alpha_j = EI\delta_j \quad (8)$$

From eqns. (1) and (3), we obtain

$$\begin{aligned} \frac{\partial M'}{\partial F_j} &= -(x - x_j) & j \leq k \\ &= 0 & j > k \end{aligned} \quad (9)$$

$$\frac{\partial M_\theta}{\partial F_j} = -(x_n - x_j + r \sin \theta)$$

Substituting eqn. (9) into eqn. (7), we have:

$$\sum_{k=1}^{n-1} \int_{x_k}^{x_{k+1}} M'(x - x_j) dx + r \int_0^{\pi/2} M_\theta(x_n - x_j + r \sin \theta) d\theta = -\alpha_j \quad (10)$$

Substituting for M' and M_θ from eqns. (1) and (3) into eqn. (10), and performing the necessary integrations, we have:

$$\begin{aligned} & \sum_{k=j}^{n-1} \left[M \left\{ \frac{x_{k+1}^2 - x_k^2}{2} - x_j(x_{k+1} - x_k) \right\} + \frac{p}{2} \left\{ \frac{x_{k+1}^4 - x_k^4}{4} - \frac{x_j(x_{k+1}^3 - x_k^3)}{3} \right\} \right. \\ & \quad \left. - \sum_{i=1}^k F_i \left\{ \frac{x_{k+1}^3 - x_k^3}{3} - (x_i + x_j) \frac{(x_{k+1}^2 - x_k^2)}{2} + x_i x_j (x_{k+1} - x_k) \right\} \right] \\ & \quad + r \left[M \left\{ (x_n - x_j) \frac{\pi}{2} + r \right\} + p x_n \left\{ \frac{\pi r^2}{4} + \frac{\pi x_n}{4} (x_n - x_j) + \frac{x_n \cdot r}{2} + r(x_n - x_j) \right\} \right. \\ & \quad \left. - \sum_{i=1}^{n-1} F_i \left\{ (x_n - x_i)(x_n - x_j) \frac{\pi}{2} + \frac{\pi}{4} r^2 + (2x_n - x_i - x_j)r \right\} \right] = -\alpha_j; \\ & \qquad \qquad \qquad j = 1, 2, \dots, (n-1) \quad (11) \end{aligned}$$

Equation (11) can be represented in subscript notation as

$$A_{ji} F_i = R_j; \quad j = 1, 2, \dots, n \quad (12)$$

where $F_n = M$; and

$$\begin{aligned} A_{ji} = & - \left[\frac{x_n^3 - x_m^3}{3} - \frac{x_i + x_j}{2} (x_n^2 - x_m^2) + x_i x_j (x_n - x_m) \right. \\ & \left. + r \left\{ (x_n - x_i)(x_n - x_j) \frac{\pi}{2} + \frac{\pi}{4} r^2 + (2x_n - x_i - x_j)r \right\} \right]; \\ & \qquad \qquad \qquad i, j = 1, 2, \dots, (n-1) \quad (13) \end{aligned}$$

where

$$m = \max(i, j) \quad (14)$$

$$\begin{aligned} R_j = & -\alpha_j - \frac{p}{2} \left[\frac{x_n^4 - x_j^4}{4} - \frac{x_j(x_n^3 - x_j^3)}{3} \right] \\ & - p r x_n \left[\frac{\pi r^2}{4} + \frac{\pi x_n}{4} (x_n - x_j) + \frac{x_n \cdot r}{2} + r(x_n - x_j) \right]; \\ & \qquad \qquad \qquad j = 1, 2, \dots, (n-1) \quad (15) \end{aligned}$$

$$A_{jn} = \frac{x_n^2 - x_j^2}{2} - x_j(x_n - x_j) + \frac{\pi r}{2} (x_n - x_j) + r^2 \quad (16)$$

Employing eqns. (4) and (6), and proceeding in a similar manner, the n th linear equation is derived:

$$M(x_n - x_1) - \sum_{k=1}^{n-1} \sum_{i=1}^k 0.5 F_i [(x_{k+1} - x_i)^2 - (x_k - x_i)^2] + \frac{p}{6} (x_n^3 - x_1^3) + r \left[\frac{\pi}{2} M - \sum_{i=1}^{n-1} F_i \left\{ \frac{\pi}{2} (x_n - x_i) + r \right\} + p x_n \left(\frac{\pi x_n}{4} + r \right) \right] = 0 \quad (17)$$

Hence the remaining coefficients of matrix A_{ij} (eqn. 12) are defined as follows:

$$A_{nj} = -\frac{1}{2} \sum_{k=j}^{n-1} [(x_{k+1} - x_j)^2 - (x_k - x_j)^2] - r \left[\frac{\pi}{2} (x_n - x_j) + r \right]; \quad j = 1, 2, \dots, (n-1) \quad (18)$$

$$A_{nn} = (x_n - x_1) + \frac{\pi r}{2} \quad (19)$$

$$R_n = -\frac{p}{6} (x_n^3 - x_1^3) - p x_n \cdot r \left(\frac{\pi x_n}{4} + r \right) \quad (20)$$

Finally, the internal moment M at $x = 0$ (vector element F_n in eqn. 12), can be eliminated from the linear equation set (12) to yield a set of $(n-1)$ linear equations, given by:

$$B_{ij} F_j = S_i; \quad i = 1, 2, \dots, n-1 \quad (21)$$

where

$$B_{ij} = \frac{A_{ij}}{A_{in}} - \frac{A_{nj}}{A_{nn}} \quad (22)$$

$$S_i = \frac{R_i}{A_{in}} - \frac{R_n}{A_{nn}} \quad (23)$$

The moment M is given by

$$M = F_n = \frac{R_n}{A_{nn}} - \frac{A_{nj}}{A_{nn}} F_j \quad (24)$$

Having thus constructed the necessary force-displacement relations for a propped pressurised obround ring, its application in obround pressure vessel design can now be discussed.

METHOD OF SOLUTION

The obround pressure vessel, as shown in Fig. 1, consists of three members, namely, (a) the obround pressure boundary, (b) longitudinal gussets and (c) anchor rings.

We focus our attention on the ring element of the obround pressure boundary located midway between the anchor rings. Traction continuity requires that the nodal point forces F_i at this element be equal to the load intensity on the gusset at this location. The gussets are modelled as elastic beams pinned at the anchor ring locations. The load intensity on a typical gusset will be symmetrical about Section A (Fig. 1) and will presumably increase from a minimum value (say F_i) at Section A to its peak value Q_i in the immediate vicinity of the anchor ring (Section B). We approximate this loading variation by a trapezoidal profile. The classical beam theory gives the midspan deflection (at Section A) of gusset i under trapezoidal loading, as:

$$\zeta_i = \frac{l^4}{E_g I_g} \left[\frac{3(Q_i - F_i)}{640} + \frac{5F_i}{384} \right] \quad (25)$$

Similarly, the net point load V_i at the anchor ring follows from force equilibrium;

$$V_i = \frac{l}{2} (F_i + Q_i) \quad (26)$$

The correct values of F_i , V_i , Q_i , δ_i , etc. are found iteratively as follows: Let Δ_i and ζ_i denote the nodal deflection of the anchor rings, and midspan beam deflection (at Section A) of the gussets. Then the nodal deflection of the pressure boundary at Section A is given by:

$$\delta_i = \zeta_i + \Delta_i \quad (27)$$

To start an iteration process, ζ_i and Δ_i are assumed zero. The iteration consists of the following steps:

- (a) Compute F_i and Q_i using eqn. (12). F_i and Q_i are nodal point forces on the pressure boundary at Sections A and B, respectively. In other words, F_i and Q_i correspond to nodal deflections δ_i and Δ_i , respectively.
- (b) Evaluate V_i and ζ_i using eqns. (26) and (25), respectively.
- (c) Compute Δ_i using eqn. (21) where the nodal forces F_j are given by V_j computed above, and the inertia properties of the anchor ring are used in the definition of α_j (eqn. 8), and Δ_j replaces δ_j .
- (d) Compute δ_i from eqn. (27). Return to step (a).

The procedure is found to converge rapidly, usually requiring no more than three to four iterations.

It is advantageous to note that the matrix $[A]$ is a function of geometric parameters only, namely the ring characteristic dimensions b and r , and nodal point

locations x_i . Thus, for a given geometry, the matrix $[A]$ has to be inverted only once. This will save substantial computational effort where a large number of iterations are required for convergence.

OBROUND RING UNDER DISTRIBUTED TWISTING MOMENT

Obround pipes require obround flanges for end closures. An inexpensive flange design, most frequently used in low and moderate pressure applications, is the so called 'Lap Joint Flange' (LJF). The LJF consists of a lap ring (Fig. 3) welded to the pipe end. The gasket is compressed over the lap ring surface by tightening the bolts against the backup ring (flange). The flange ring may be made of inexpensive materials, e.g. low-alloy steel plate or forgings, since it does not come in direct contact with the contained fluid.

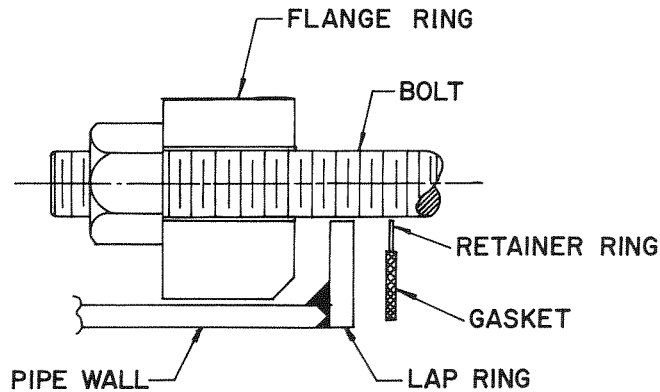


Fig. 3. Lap joint flange cross section.

The design method for circular lap joint flanges is well known.¹ In what follows, we will devise equivalent design formulae for obround cross-section flanges. Following the procedure given in reference 1, the loadings applied on a lap joint flange may be approximated by a uniformly distributed couple m . Furthermore, it is assumed here that the characteristic dimensions of the ring cross-section are small compared to its arc radius r .

The total strain energy, U , contained in the ring is given by:

$$U = \oint \frac{T^2 ds}{2GI_p} + \oint \frac{M^2 ds}{2EI} \quad (28)$$

where T and M are internal torque and moment, and G and I_p are shear modulus and polar moment of inertia of the ring, respectively. Let T_0 and M_0 be the unknown

moments at point A ($x = 0$) in Fig. 4. Appealing to Castigliano's theorem, it can be shown that:

$$T_0 = 0$$

and (29)

$$M_0 = mr$$

where m = applied twisting moment per unit perimeter. The moment M and torque T at any point are now statically determinate. At a point on the straight segment:

$$T = -mx$$

$$M = mr; \quad x \leq b \quad (30)$$

Similarly, on the curved segment; at point B,

$$T = mb \sin \theta$$

$$M = m[r - b \cos \theta] \quad (31)$$

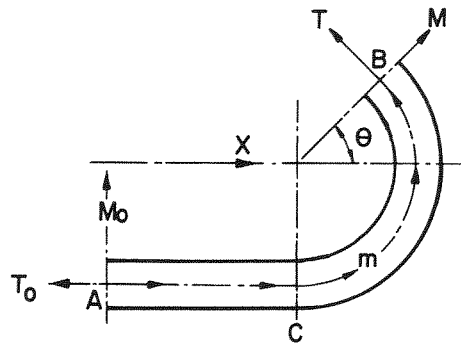


Fig. 4. Obround ring under a uniform twisting moment.

From eqns. (30) and (31) it is obvious that the most stressed point is the junction of the straight segment with the curved portion, point C. Using the properties of the cross section, and eqn. (24), the maximum stress at point C ($x = b$) can be readily determined. Or conversely, the required ring cross section can be found for specified allowable stress limits.

EXAMPLE

To illustrate the influence of gusset location, we consider an obround ring of unit width, $b = 39.69$ cm (15.63 in); $r = 34.61$ cm (13.63 in), subjected to an internal pressure of 2.109 kg/cm² (30 psi). A total of 6 gussets are to be arranged such as to

minimise the bending stresses. For purposes of illustration we assume the gussets to be inflexible. Locating the gussets symmetrically with respect to the pipe cross-section (Fig. 5), the distance parameter $\eta = b_1/b$, is the unknown quantity of interest. Figure 5 shows the bending moment M' as a function of x/b for $\eta = 0.5$, 0.768 and 1 . It is obvious from Fig. 5 that η has a very significant effect on the magnitude and location of the maximum bending stress. For example, for $\eta = 0.768$, the maximum bending moment is 55.5% of the value for $\eta = 1$. This means that for $\eta = 0.768$ the pipe has to be only about 74.5% of its required thickness for $\eta = 1$.

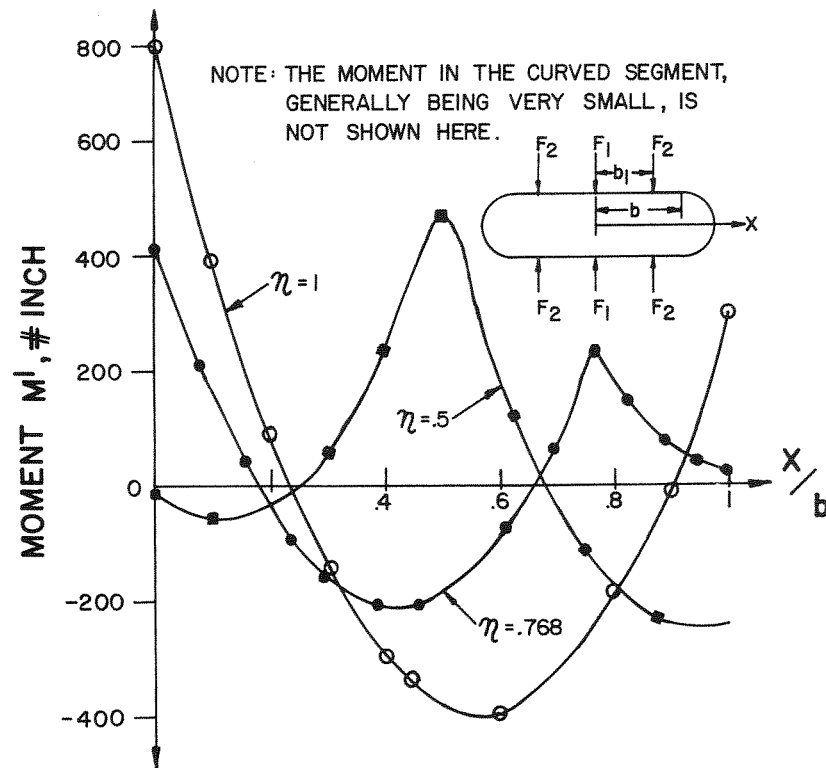


Fig. 5. Moment M' as a function of x/b .

CONCLUSION

A method to efficiently design a pressurised obround pipe with multiple gusset supports has been devised. The solution is developed for the two-dimensional model (plane stress) assuming two axes of symmetry. The symmetry requirement is

imposed here because the asymmetrical cases are hardly of any practical interest. It is shown that the locations of the support gussets have a profound influence on the maximum stresses developed. To achieve maximum economies in material and fabrication, it is desirable to determine the 'optimal' gusset locations. The method prescribed in this paper enables a designer to arrive at the most desirable design with a minimum of computation effort. The formulae for designing obround lap joint flanges are also given.

The prescription proposed in this paper makes no pretence to a rigorous analysis of the elasticity problem. Instead a design oriented engineering solution is sought which concentrates on the dominant stress components while neglecting the less important ones to simplify analysis. In particular, the bending stress in z -direction (Fig. 1), developed due to elastic deflection of gussets between anchor points, is neglected, which enabled the pipe to be treated as a planar ring.

In industrial practice, the use of the obround cross section pipes will remain limited to special purpose applications such as the ones cited before. For example, the nozzles of a reboiler and a column may have to be made obround; but their interconnecting piping, if long, will be circular. Thus, in essence, the obround pipes are normally short, seldom exceeding 2-3 feet in length. In such short lengths, proper reinforced vessel wall opening and the nozzle end flange act as two anchor rings, and any additional intermediate anchor rings may not be needed.

Finally, this paper is not concerned with the discontinuity stresses due to interaction of pipe ends with vessel openings. This problem, to the best of our knowledge, still remains analytically intractable.

REFERENCES

1. ASME Boiler and Pressure Vessel Code, Section VIII, Division I, Paragraph UG-36. The American Society of Mechanical Engineers, New York (1974), pp. 28 and 233-60.
2. DEN HARTOG, J. P. *Advanced Strength of Materials*, McGraw Hill, New York (1952) p. 212.
3. SOKOLNICOFF, I. S. *Mathematical Theory of Elasticity*, McGraw Hill, New York (1956) p. 84.
4. *Scientific Subroutine Package, System/360 (360 4-CM-03 X) Version III, Programmer's Manual, H20-0205-2*, IBM Corp., White Plains, N.Y. (1968) pp. 121-23.
5. ASME Boiler and Pressure Vessel Code, Section III, Division I, Subsection NA, Appendix XIII, The American Society of Mechanical Engineers, New York (1974) p. 325.